Pergamon

0045-7949(94)00394-7

Computers & Structures Vol. 54, No. 6, pp. 1113–1126, 1995

0045-7949/95 $9.50 + 0.00

A SIMPLIFIED DAMAGE MECHANICS APPROACH TO NONLINEAR ANALYSIS OF FRAMES

A. Cipollina, A. López-Inojosa and **J. Flórez-López**
Facultad de Ingeniería, Universidad de Los Andes, Mérida, Venezuela

(*Received* 31 *October* 1993)

Abstract—This paper presents a general formulation for frame analysis based on 'lumped dissipation models' and continuum damage mechanics. A particular model for RC frames based on this framework is proposed and the numerical implementation of simplified damage models in commercial finite element programs is described.

1. INTRODUCTION

Since the pioneering paper of Kachanov [1], continuum damage mechanics has become one of the most active fields of research in solid mechanics. The main idea is the introduction of a new internal variable, the damage, that measures the density of microcracks and microvoids and their influence on the behavior of the material. This basic idea is so simple and so general that it has been used for the modeling, until local fracture, of most construction materials (see, for instance, [2] and its references).

However continuum mechanics is not the most suitable framework for the analysis of many civil engineering structures. These are often modeled as trusses or fames because continuum models can be used only for relatively simple structures.

Plasticity theories have been successfully adapted to frame analysis through the notion of 'lumped plasticity models', in which it is assumed that plastic effects can be concentrated in special locations called 'plastic hinges' (see [3–5] and its references).

As a result of studies carried out in the University of the Andes, Venezuela, in the area of nonlinear frame analysis [6–10], a formulation that generalizes the lumped plasticity models to include damage effects is proposed. This formulation can be considered as simplified damage mechanics or fracture mechanics for frames; that is a theory for frame analysis that incorporates some notions and methods of continuum damage mechanics and fracture mechanics. A numerical formulation for the resolution of damageable frames is also proposed. The main advantage of this formulation is that it allows the implementation of simplified damage models in standard finite element programs. A mathematical analysis of the problem is not considered in this paper; therefore, uniqueness, stability and localization in simplified damage models are not studied. However, we are aware that these are fundamental problems arising in strain-softening and damage-softening models. For the sake of simplicity we consider only planar frames in quasi-static conditions. Although this formulation can easily be generalized, experimental identification of the model in the three-dimensional case could be difficult.

This paper is organized as follows: in Sections 2 and 3 the notation that is used in the paper is presented. In Section 4 a general framework for plasticity, coupled to damage for planar frames, is introduced and a particular model for RC frames is identified. In Section 5 the numerical analysis of these simplified models is described and some numerical examples are presented in Section 6.

2. KINEMATICS OF PLANAR FRAMES

2.1. *Notation*

Let us consider a planar frame of 'm' members connected by 'n' nodes. The latter are grouped into two sets: $\mathbf{N}_\sigma$ and $\mathbf{N}_u$; $\mathbf{N}_\sigma$ contains the nodes subjected to external loads and $\mathbf{N}_u$ includes the 'supports' of the structure, i.e. the nodes where displacements are imposed. We study the movement of the structure during a time interval $[0, T]$. The state of the structure at time t equal to zero is denoted 'initial or undeformed configuration'. For t greater than zero, any configuration of the structure is called 'deformed'.

We introduce a couple of orthogonal coordinate axes: X and Y, to define the position of each node at any configuration. This coordinate system remains stationary during the movement of the structure.

We define now the following variables ($\{\bullet\}$ indicates a column matrix and $\{\bullet\}^t$ is its transposed form):

(a) Generalized displacements of a node 'i' are denoted by $\{U\}_i^t = (u_1, u_2, u_3)$, where u_1, and u_2 are, respectively, the displacements in the X and Y directions; u_3 indicates the rotation of the node with respect to the position of the node in the initial configuration (Fig. 1).

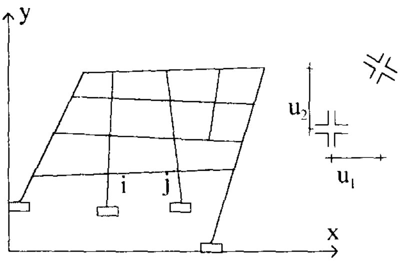

Fig. 1. Generalized displacements of a node 'i'.

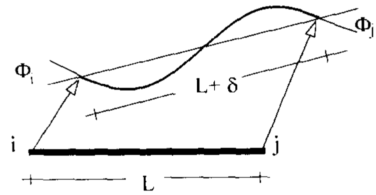

Fig. 2. Generalized deformations of a member between nodes 'i' and 'j'.

(b) Generalized displacements of a member 'b' between nodes 'i' and 'j' are denoted by: $\{q\}^t = (\{U\}_i^t, \{U\}_j^t)$. Alternatively, we will use the notation $\{q\}_b$ to indicate the displacements of the same member 'b', but zeros will be added at the positions that correspond to the degrees of freedom of the other nodes of the structure, i.e.

$$\{q\}_b^t = (\underset{\text{node 1}}{(0,0,0)}, \underset{\text{node 2}}{(0,0,0)}, \dots, \underset{\text{node } i}{\{U\}_i^t}, \underset{\text{node } i+1}{(0,0,0)}, \dots, \underset{\text{node } j}{\{U\}_j^t}, \dots, \underset{\text{node } n}{(0,0,0)}). \tag{1}$$

(c) Generalized displacements of the structure are denoted by

$$\{X\}^t = (\{U\}_1^t, \{U\}_2^t, \dots, \{U\}_h^t). \tag{2}$$

(d) Generalized deformations of a member 'b' between nodes 'i' and 'j', denoted by $\{\Phi\}^t = (\Phi_i, \Phi_j, \delta)$, where Φ_i and Φ_j indicate, respectively, rotations of the member at the ends 'i' and 'j' with respect to the cord 'i–j' (Fig. 2) and δ is the elongation of the cord with respect to its length in the initial configuration.

2.2. *Compatibility equations*

Deformation and member displacement rates are related by the following expression:

$$\{\dot{\Phi}\} = [B(t)]\{\dot{q}\}, \tag{3}$$

where displacement transformation matrix $[B(t)]$ is a function of the deformed configuration (Appendix A). Compatibility equations are obtained by integration of (1) from the initial configuration to the deformed configuration at time t:

$$\{\Phi\} = \int_0^t [B(\tau)]\{\dot{q}\}\, d\tau. \tag{4a}$$

This integration can be performed explicitly (Appendix B).

If displacements are small, the displacement transformation matrix remains constant, i.e. $[B(t)] \cong [B^0]$ where the latter is the displacement matrix in the undeformed configuration. In such a case, eqn (4a) becomes

$$\{\Phi\} = [B^0]\{q\}. \tag{4b}$$

3. GENERALIZED STRESSES AND INTERNAL FORCES

3.1. *Notation*

(a) Generalized internal forces on a member 'b' are denoted by $\{Q\}^t = (Q_1, Q_2, \dots, Q_6)$ (Fig. 3) or the matrix $\{Q\}_b$ built in the same way as $\{q\}_b$.

(b) We introduce the 'generalized stresses' of a member $\{M\}^t = (M_i, M_j, N)$, that is conjugated with respect to generalized deformations $\{\Phi\}$; M_i and M_j are the moments on the ends of the member and N represents the axial force (Fig. 3).

(c) We assume that the structure is subjected to concentrated forces and moments on the nodes. These external actions are grouped into a matrix $\{P\}$:

$$\{P\}^t = (\underset{\text{actions on node 1}}{(p_1, p_2, p_3)}, \dots, \underset{\text{actions on node } n}{(p_{3n-2}, p_{3n-1}, p_{3n})}) \tag{5}$$

This matrix contains external forces as well as reactions on supports.

3.2. *Equilibrium equations*

(a) Static equilibrium of the members determine the relation between internal forces and generalized stresses at deformed configurations:

$$\{Q\} = [B(t)]^t\{M\}. \tag{6a}$$

If displacements are small, then we have, in any configuration,

$$\{Q\} = [B^0]^t\{M\}. \tag{6b}$$

(b) Quasi-static equilibrium of the nodes is expressed as

$$\{P\} - \sum_{b=1}^{m} \{Q\}_b = 0. \tag{7}$$

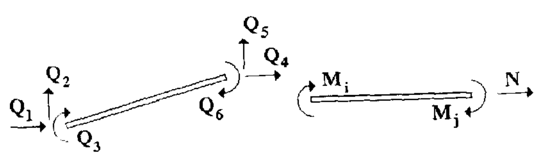

Fig. 3. Internal forces and generalized stresses of a member.

4. CONSTITUTIVE EQUATIONS

4.1. *Lumped dissipation model*

Relations between generalized stresses and the history of deformations must be included in order to completely define the problem. If the member has an elastic behavior this relation is expressed as follows:

$$\{M\} = [S^e(\Phi)]\{\Phi\} \quad \text{or} \quad \{\Phi\} = [F^e(M)]\{M\}, \tag{8a}$$

where $[S^e(\Phi)]$ and $[F^e(M)]$ denote, respectively, the local elastic stiffness and flexibility matrices. They are a function of the deformed configuration of the member (Appendix C).

If deformations are small, then the stiffness and flexibility matrices remain constant. In such a case, we can write the elastic constitutive equation as follows:

$$\{M\} = [S^0]\{\Phi\} \quad \text{or} \quad \{\Phi\} = [F^0]\{M\}. \tag{8b}$$

Under severe overloads, the elastic model is obviously inadequate because the member may undergo plasticity, damage (cracking of the concrete in RC frames, for instance), hardening and other energy-dissipation phenomena. A more general constitutive equation can be obtained using the 'lumped dissipation model' of the member indicated in Fig. 4. The member is characterized as the assemblage of an elastic beam-column and two zero-length inelastic hinges at the end of the member. This representation is similar to the 'lumped plasticity model' used commonly to elaborate plasticity theories for frames [3–5]. In this paper, it is called 'lumped dissipation' instead of 'lumped plasticity' since damage and other inelastic effects are being taken into account. Energy dissipation is assumed to concentrate only in the hinges while beam-column behavior always remains elastic. Member deformations can now be expressed as

$$\{\Phi\} = [F^e]\{M\} + \{\Phi^h\}. \tag{9}$$

The first term of the right-hand part of (9) corresponds to the beam-column deformations where the symbol $[F^e]$ is the flexibility matrix introduced in (8), the last term is called 'hinge deformation'.

We assume that hinge deformations result from plastic deformations, as defined in standard plastic theories for frames, and an additional term due to damage

$$\{\Phi^h\} = \{\Phi^p\} + \{\Phi^d\}. \tag{10}$$

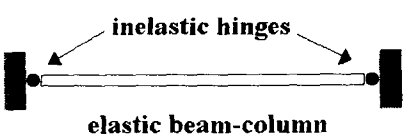

Fig. 4. Lumped dissipation model of a member.

An expression for damage deformations $\{\Phi^d\}$, based on the results of continuum damage mechanics, is proposed in Section 4.3.

4.2. *Elements of continuum damage mechanics*

Continuum damage mechanics (see [2] for a general presentation) is based on the introduction of a new internal variable, that characterizes a surface density of microcracks and microvoids: let A_d be the area of microdefects, including stress concentration effects, of a representative volume element and A, its total nominal area. Then damage is defined as

$$D = \frac{A_d}{A}. \tag{11}$$

Damage can take values between zero (intact element) and one (broken element). Obviously damage has an influence on the elastic behavior of the material; this is taken into account through the 'effective stress' notion and the 'strain equivalence' hypothesis. Effective stress $\bar{\sigma}$ is defined as the ratio between the load applied on the volume element and the 'effective resistance area' $\bar{A} = A - A_d$. Therefore, the relation between effective stress and Cauchy stress is given by

$$\bar{\sigma} = \frac{\sigma}{(1-D)}. \tag{12}$$

The hypothesis of strain equivalence consists of assuming that if we substitute Cauchy stress by effective stress, the behavior of a damaged material is the same as an intact material, i.e.

$$\epsilon^e = \frac{\bar{\sigma}}{E} = \frac{\sigma}{E(1-D)}, \tag{13}$$

where ϵ^e is the elastic strain and E the elastic stiffness of the intact material.

Constitutive equations in damage mechanics are obtained by adding damage evolution laws to eqn (13). These laws are identified from experimental results and are material dependent [2].

4.3. *Flexibility matrix of a damaged member*

Let us first consider the particular case of a truss member in the small displacement case. Then only axial generalized stress and deformation has to be taken into account. In such a case, on one hand, it follows from (13) (assuming that the state of damage is constant and that there is no localization in the member) that

$$\delta = \frac{N}{(1-D)S_{33}^0} + \delta^p, \quad \text{where} \quad S_{33}^0 = EA/L. \tag{14}$$

On the other hand, in lumped dissipation models the elongation δ of the member is given by (see expressions (9) and (10))

$$\delta = \frac{N}{S_{33}^0} + \delta^p + \delta^d. \tag{15}$$

From (14) and (15) we obtain

$$\delta^d = \frac{D}{(1-D)S_{33}^0} N. \tag{16}$$

This equation means that in order to have a lumped dissipation model with the same behavior of a truss member in continuum damage mechanics, it is necessary to define the damage axial deformation of the hinges by (16). For D equal to zero (no damage), we have axial hinges with zero flexibility of infinity stiffness (a rigid-plastic member). When D takes the value one, we obtain a member with infinite axial flexibility or zero stiffness (hinges and elastic beam are unconnected).

where

$$[F^d(M, D)] = [F^e(M)] + [C(D)]. \tag{18}$$

The term $[F^d(M, D)]$ represents the flexibility matrix of a damaged member. Parameters d_i and d_j respectively measure flexion damage of hinges 'i' and 'j'. Parameter d_n is the measure of 'axial damage' of the member. In the particular case of a truss where M_i and M_j take the value zero, we obtain the standard damage mechanics state law (14) with $d_n = D$.

If a flexion damage parameter takes the value zero (no damage) we have a plastic hinge like that of a standard lumped plasticity models. If it takes the value one (totally damaged) the hinge will be denoted 'totally damaged hinge' and has the same behavior as an internal hinge in an elastic frame.

As an example, the stiffness matrix of a member of inertia 'I' area 'A' and length 'L' in the small displacements case is shown:

$$[S^d(D)] = \begin{bmatrix} \dfrac{(1-d_i)(4-d_j)}{4-d_i d_j} 4EI/L & \dfrac{4(1-d_i)(1-d_j)}{4-d_i d_j} 2EI/L & 0 \\ & \dfrac{(1-d_j)(4-d_i)}{4-d_i d_j} 4EI/L & 0 \\ \text{sym.} & & (1-d_n)AE/L \end{bmatrix}. \tag{19}$$

A similar analysis cannot be made in the presence of flexural or large displacements effects, even with very simple damage evolutions laws. Therefore we postulate the existence of a set of damage parameters $\{D\}^t = (d_i, d_j, d_n)$ which can take values in the interval [0, 1], so that the behavior of the hinges is given by:

$$\{\Phi^d\} = [C(D)]\{M\}, \tag{17}$$

where

$$[C(D)] = \begin{bmatrix} \dfrac{d_i}{(1-d_i)S_{11}^0} & 0 & 0 \\ 0 & \dfrac{d_j}{(1-d_j)S_{22}^0} & 0 \\ 0 & 0 & \dfrac{d_n}{(1-d_n)S_{33}^0} \end{bmatrix}.$$

This relation was proposed in [6].

Equations (9) and (10) and (17) define the generalized stress-deformation relation for a damageable elasto-plastic member. From these relations it follows

$$\{\Phi - \Phi^p\} = [F^d(M, D)]\{M\},$$

It can be seen that for $\{D\}$ equal to zero, we obtain the standard stiffness matrix of an elastic member. If d_i is equal to one and the other damage parameters take the value zero then $[S^d(D)]$ becomes the stiffness matrix of an elastic member with an internal hinge at the left end. When both flexural damage parameters are equal to zero, we have the stiffness matrix of an elastic truss bar.

4.4. *Thermodynamic forces conjugated to damage and other internal variables*

Complementary potential energy of a damaged member U^* is given by

$$U^*(M, D) = \tfrac{1}{2}\{M\}^t[C(D)]\{M\} + W^*, \tag{20}$$

where the first term is the contribution of the hinges to the complementary potential energy and W^* represents the complementary potential energy of the elastic beam-column. We assume that free enthalpy of a member can be expressed as the sum of the complementary potential energy plus an additional plastic potential that depends on set internal variables:

$$\{\alpha\}^t = (\alpha_1, \alpha_2, \ldots):$$

$$\chi = U^*(D, M) + U^p(\alpha). \tag{21}$$

Parameters α_i may correspond to kinematic or isotropic plastic hardening variables. State law (17) can now be obtained as

$$\{\Phi^e\} = \{\Phi - \Phi^p\} = \left\{\frac{\partial \chi}{\partial M}\right\}. \tag{22}$$

Thermodynamic forces conjugated to damage can be defined in a similar way:

$$\{G\} = -\left\{\frac{\partial \chi}{\partial D}\right\}. \tag{23}$$

These forces are the equivalent of the energy release rate introduced in fracture and continuum damage mechanics. They have the following explicit expression:

$$G_i = -\frac{\partial \chi}{\partial d_i} = \frac{1}{2S_{11}^0}\left[\frac{M_i}{(1-d_i)}\right]^2$$

$$G_j = -\frac{\partial \chi}{\partial d_j} = \frac{1}{2S_{22}^0}\left[\frac{M_i}{(1-d_j)}\right]^2$$

$$G_n = -\frac{\partial \chi}{\partial d_n} = \frac{1}{2S_{33}^0}\left[\frac{N}{(1-d_n)}\right]^2. \tag{24}$$

Thermodynamic forces conjugated to plastic hardening parameters $\{\alpha\}$ are given by

$$\{\beta\} = -\left\{\frac{\partial \chi}{\partial \alpha}\right\}. \tag{25}$$

Energy dissipation due to damage and plasticity is now given by

$$\xi = \{\dot{D}\}^t\{G\} + \{\dot{\Phi}^p\}\{M\} + \{\dot{\alpha}\}\{\beta\} \geqslant 0. \tag{26}$$

Energy dissipation must be positive because of the laws of thermodynamics. If we assume that energy dissipation mechanisms are independent (possibility of damage without plasticity and vice versa) then each of them must be positive, i.e.

$$\dot{\Phi}_i^p M_i + \dot{\delta}^p N + \text{hardening terms (hinge } i) \geqslant 0$$

$$\dot{\Phi}_j^p M_j + \dot{\delta}^p N + \text{hardening terms (hinge } j) \geqslant 0$$

$$\dot{d}_i G_i + \dot{d}_n G_n + \text{hardening terms (hinge } i) \geqslant 0$$

$$\dot{d}_j G_j + \dot{d}_n G_n + \text{hardening terms (hinge } j) \geqslant 0. \tag{27}$$

These inequalities can be used during numerical calculations to identify elastic unloading.

4.5. *Internal variable evolution laws*

Internal variable evolution laws are now introduced so that standard lumped plasticity models are obtained if damage remains constant ($\{\dot{D}\} = 0$).

The following general expressions were proposed in [10]:

(a) Plastic deformation evolution laws:

$$\dot{\Phi}_i^p = \dot{\lambda}_i^p \frac{\partial f_i}{\partial M_i} \quad \dot{\Phi}_j^p = \dot{\lambda}_j^p \frac{\partial f_j}{\partial M_j}$$

$$\dot{\delta}^p = \dot{\lambda}_i^p \frac{\partial f_i}{\partial N} + \dot{\lambda}_j^p \frac{\partial f_j}{\partial N} \tag{28}$$

where $f_i \leqslant 0$ and $f_j \leqslant 0$ are respectively the yield or plastic functions of hinges 'i' and 'j'. These functions depend on the generalized stresses $\{M\}$ and may depend on the internal variables and plastic multiplicators λ_i^p and λ_j^p. They must become the standard yield functions of plastic models when damage parameters remain constant. Plastic multipliers are calculated in the usual manner:

$$\dot{\lambda}^p \begin{cases} = 0 & \text{if } f < 0 \quad \text{or} \quad f < 0 \text{ (no plasticity)} \\ \neq 0 & \text{if } f = 0 \quad \text{and} \quad f = 0 \text{ (plastic increment).} \end{cases} \tag{29}$$

Plastic deformation will be called 'active' in a hinge if the corresponding plastic multiplier is strictly positive, otherwise it will be called 'passive'.

(b) Damage evolution laws:

$$\dot{d}_i = \dot{\lambda}_i^d \frac{\partial g_i}{\partial G_i} \quad \dot{d}_j = \dot{\lambda}_j^d \frac{\partial g_j}{\partial G_j}$$

$$\dot{d}_n = \dot{\lambda}_i^d \frac{\partial g_i}{\partial G_n} + \dot{\lambda}_j^d \frac{\partial g_j}{\partial G_n}, \tag{30}$$

where $g_i \leqslant 0$ and $g_j \leqslant 0$ are called 'damage functions' and have the same role as the plastic functions, i.e. they indicate if a damage process has taken place in a member. Damage functions depend on thermodynamic forces associated to damage. They may depend on the internal variables and 'damage multipliers' λ^d. The latter are calculated as the plastic multipliers:

$$\dot{\lambda}^d \begin{cases} = 0 & \text{if } g < 0 \quad \text{or} \quad g < 0 \text{ (no damage)} \\ > 0 & \text{if } g = 0 \quad \text{and} \quad g = 0 \text{ (damage increment).} \end{cases} \tag{31}$$

As in the previous case, damage is 'active' in a hinge if the corresponding damage multiplier is strictly positive, otherwise it is 'passive'.

If other internal variables $\{\alpha\}$ are present in the model, then their evolution laws can also be obtained from the plastic or damage functions or independent yield functions by the normality rule.

4.6. *Evolution law identification*

Plastic and damage functions and, in some cases, U^p are the only terms that must be determined in order to completely define the model. The

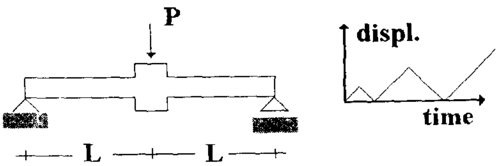

Fig. 5. Test for yield function identification: specimen and loading.

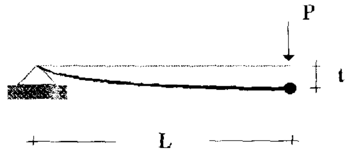

Fig. 7. Lumped dissipation model of the test.

material of the member has not yet been taken into account. These functions are specific for each kind of frame (RC, steel and so on). Plastic and damage functions can be obtained from experimental results, as in lumped plasticity models and phenomenological models of continuum mechanics. This identification can be performed with civil engineering standard tests on beam-column joints. As an example, a procedure for evolution law identification that was applied to the particular case of RC members under reversible (but not cyclic loading) is presented.

Figure 5 shows a scheme of a specimen that represents a beam-column joint. The loading of the test is indicated in the same figure. The results of one of the tests are summarized in the curve force–displacement of Fig. 6. The characteristics of this specimen are $L = 0.705$ m, $A = 15 \times 20\,\mathrm{cm}^2$, Reinforcement $4\phi 9.525$ mm(3/8′), $f_c \cong 25\,\mathrm{N/mm}^2$, $f_y \cong 420\,\mathrm{N/mm}^2$.

The lumped dissipation model of the test is shown in Fig. 7. The specimen of Fig. 5 is represented by two members but due to the symmetry of the structure only one of the members is shown in Fig. 7. Small displacements and deformations are assumed. Asymmetric bifurcation with respect to the fundamental solution is possible, however we assume that this can appear only when the specimen exhibits softening behavior. Therefore only the values up to the peak of the displacement–force curve are used for model identification. Only one inelastic hinge appears in the member of Fig. 7 because we assume that d_i and Φ_i^p are equal to zero (The moment is equal to zero in the left end.) We assume that d_n, δ and δ^p are equal to zero too because there is no axial force. Then, taking into account (4b), (18) and (19), we have

$$P = \frac{4-4d}{4-d}\left(\frac{6EI}{L^3}\right)(t - t^p) = Z(d)(t - t^p), \tag{32}$$

where t indicates the deflection of the mid-point of the specimen, P is the force applied on the specimen, $d = d_j$ and $t^p = L\Phi_j^p$.

The series of loading and unloading allows for the experimental determination of the elastic stiffness Z and the plastic deflection t^p at different values of the forces P. These terms have, in the lumped dissipation model of the test, the following expressions:

$$Z = \frac{4-4d}{4-d}Z_0; \quad Z_0 = \left(\frac{6EI}{L^3}\right); \quad t^p = L\Phi_j^p. \tag{33}$$

These relations and the experimental values of Z and t^p allow the measurement of the damage parameter 'd' and the plastic deformation 'Φ^p' at the time of each unloading (assuming that no further damage and plasticity effects happen until reloading):

$$d = 4\left(1 - \frac{Z}{Z_0}\right)\Big/\left(4 - \frac{Z}{Z_0}\right); \quad \Phi^p = \frac{t^p}{L}. \tag{34}$$

The measures of M and G (the conjugated variables of Φ^p and d) are given by

$$M = \frac{PL}{2}; \quad G = \frac{L}{8EI}\left(\frac{M}{1-d}\right)^2. \tag{35}$$

The curves M as a function of Φ^p and d as a function of G are shown in Figs 8 and 9. Plastic and damage

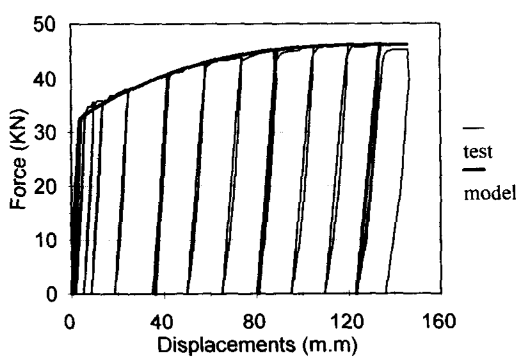

Fig. 6. Displacement vs force in the identification test.

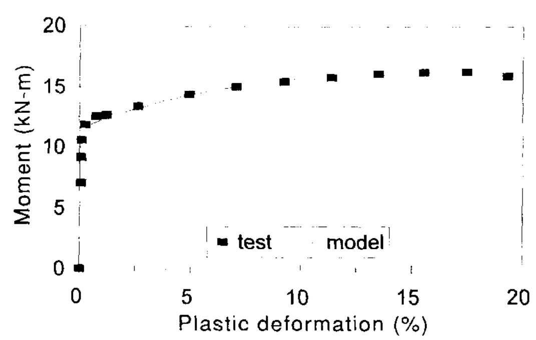

Fig. 8. Generalized stresses as a function of plastic deformations.

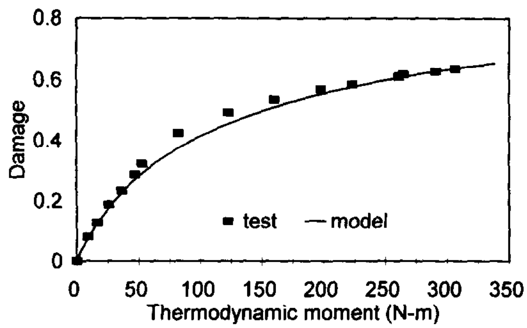

Fig. 9. Damage as a function of its thermodynamic moment.

functions were identified from these curves and other similar tests [7]. We propose the following expressions:

$$f = \left| M - \left(\frac{1-d}{4-d}\right) c\Phi^p \right| - 4\left(\frac{1-d}{4-d}\right) M_y$$

$$g = G - \left(G_{cr} + q \frac{\ln(1-d)}{(1-d)} \right). \quad (36)$$

where c, M_y, G_{cr} and q are constants that characterize the member. A comparison between the tests and the models are indicated in Figs 6, 8 and 9. Only three unloadings are indicated in the curve corresponding to the model in Fig. 9 but similar results are obtained for every unloading.

It can be noticed that these constitutive equations become the perfect elasto–plastic model if damage remains constant and c takes the value zero. If c is positive, but there is no damage increments, we obtain a bilinear elasto–plastic model with kinematic hardening. In the general case, the 'size' of the elastic zone is given by the competition between the hardening produced by plasticity and the softening due to damage.

The damage function exhibits an initial 'non-damage' zone of size G_{cr} and a 'hardening' term given by the last parenthesis of the damage function. If q takes the value zero the damage evolution would be the equivalent of the Griffith criterion, introduced in fracture mechanics, for frames.

Parameters c, M_y, G_{cr} and q have non-well-defined mechanical interpretations. Rather than determine these constants directly, it is preferable to calculate them by the numerical resolution of the following non-linear system of equations:

$$M = M_{cr} \quad \text{implies } d = 0$$

$$M = M_p \quad \text{implies } \Phi^p = 0$$

$$M = M_u \quad \text{implies } \frac{dM}{d\Phi^p} = 0,$$

$$M = M_u \quad \text{implies } \Phi^p = \Phi^p_u, \quad (37)$$

where M_{cr} is the cracking moment, M_p is the yield or plastic moment, M_u the ultimate moment and Φ^p_u is the plastic deformation at the ultimate moment. Numerical resolution of (37) can be performed by standard methods. These parameters can be obtained from classic theory of reinforced concrete (see, for instance [11]) or by more sophisticated methods that will not be discussed in this paper. We assume that these coefficients can be estimated when the characteristics of the member are known (length, area of the cross-section, amount and distribution of the reinforcement, properties of the concrete and so on). Obviously the performance of the model depends on the quality of the methods used for their calculation. In the numerical simulations indicated in Figs 6, 8 and 9 these values were taken from the experimental results, which explains the excellent agreement between model and experiment. These values were $L = 0.705$ m, $S_0 = 3286$ kN-m, $M_u = 16.29$ kN-m, $M_p = 11.50$ kN-m, $M_{cr} = 0$, $\Phi_{pu} = 0.174822$.

More sophisticated models for cyclic loading based on the same framework are under development [12].

5. NUMERICAL ANALYSIS OF SIMPLIFIED DAMAGE MODELS

5.1. *Formulation of the problem*

Given:

(a) The geometry of the structure defined by nodes coordinate and the connection table that defines the members.

(b) Properties of the members.

(c) Loading history of the nodes belonging to the set $\mathbf{N}_\sigma$ during the time interval $[0, T]$.

(d) Displacement history of the nodes in the set $\mathbf{N}_u$ during the same interval.

Calculate:

(a) Displacement history $\{X(t)\}$ of the nodes in $\mathbf{N}_\sigma$.

(b) Reactions on the nodes in $\mathbf{N}_u$.

(c) Deformations $\{\Phi(t)\}$, stresses $\{M(t)\}$, internal forces $\{Q(t)\}$, plastic deformations $\{\Phi^p(t)\}$, damage $\{D(t)\}$, thermodynamic forces $\{G(t)\}$ and, if necessary, the remaining internal variables and their associated forces $\{\alpha(t)\}$, $\{\beta(t)\}$ for each member of the structure.

Such that they verify:

(a) Compatibility eqns (4).

(b) Equilibrium eqns (6) and (7).

(c) State laws (18), (24) and (25).
(d) Internal variables evolution laws (28)–(31).

5.2. *Time discretization*

Time interval $[0, T]$ is discretized into $(0, t_1, t_2, \ldots t_r, \ldots, T)$. The unknowns of the problem are not calculated during the entire history but only at the times t_r by a standard step-by-step method. Time derivatives appear only in the internal variables evolution laws. These relations must then be discretized. It can be done by the following 'θ-method':

Let $\{A\}' = (A_i, A_j, A_n)$ be the values at the end of a step of any internal variable, i.e. $\{A\}$ may represent plastic deformations or damage. Let $\{Y\}' = (Y_i, Y_j, Y_n)$ be the conjugated force to $\{A\}$, i.e. generalized stress or thermodynamic forces associated to damage. Values at the beginning of the step are denoted by $\{A_0\}$ and $\{Y_0\}$. Increments of these variables during the step are $\{\Delta A\}$ and $\{\Delta Y\}$, where

$$\{\Delta A\} = \{A\} - \{A_0\}; \quad \{\Delta Y\} = \{Y\} - \{Y_0\}. \quad (38)$$

Evolution of $\{A\}$ is determined by yield functions 'h_i' for hinge 'i' and 'h_j' for hinge 'j', i.e. they can represent plastic or damage functions. Inelastic multipliers associated with functions 'h' are denoted, respectively, as λ_i and λ_j. Then increments of the internal variable $\{A\}$ can be approximated as follows:

$$\begin{aligned} \Delta A_i &= \Delta\lambda_i \left.\frac{\partial h_i}{\partial Y_i}\right|_{\{A\}=\{A_\theta\};\{Y\}=\{Y_\theta\}} \\ \Delta A_j &= \Delta\lambda_j \left.\frac{\partial h_j}{\partial Y_j}\right|_{\{A\}=\{A_\theta\};\{Y\}=\{Y_\theta\}} \\ \Delta A_n &= \Delta\lambda_i \left.\frac{\partial h_i}{\partial Y_n}\right|_{\{A\}=\{A_\theta\};\{Y\}=\{Y_\theta\}} \\ &\quad + \Delta\lambda_j \left.\frac{\partial h_j}{\partial Y_n}\right|_{\{A\}=\{A_\theta\};\{Y\}=\{Y_\theta\}}, \end{aligned} \quad (39)$$

where $\{A_\theta\} = \theta\{A\} + (1-\theta)\{A_0\}$; $0 \leqslant \theta \leqslant 1$; and $\{Y_\theta\}$ is defined in the same way.

This implicit (when $\theta \neq 0$) integration scheme is similar to others used in continuum damage mechanics. For a stability analysis of this algorithm see [13].

After discretization, the equation that allows the determination of the increment of the inelastic multiplier becomes

$$\begin{cases} h_i = 0 & \text{if the internal variable } \{A\} \text{ is active in hinge '}i\text{'} \\ \Delta\lambda = 0 & \text{otherwise.} \end{cases} \quad (40)$$

Energy dissipation inequality (27) due to the evolution of $\{A\}$ can be written as

$$Y_{i\theta}\Delta A_i + Y_{n\theta}\Delta A_n \geqslant 0 \quad Y_{j\theta}\Delta A_j + Y_{n\theta}\Delta A_n \geqslant 0. \quad (41)$$

Equations (39) and (40) (specified for each internal variable of the constitutive model) must substitute the internal variable evolution laws (28)–(31), in order to solve numerically the problem formulated in Section 5.1. Inequalities (41) can be used to identify elastic unloading.

5.3. *Formulation of the global and local problems*

Compatibiltiy eqns (4), member equilibrium eqns (6) and constitutive eqns (18), (24), (39) and (40) constitute a nonlinear matrix system of 10 equations with 11 unknowns ($\{q\}$, $\{\Phi\}$, $\{\Phi^p\}$, $\{D\}$, $\{M\}$, $\{G\}$, $(\lambda_i^p, \lambda_j^p)$, $(\lambda_i^d, \lambda_j^d)$; $\{\alpha\}$ and $\{\beta\}$ if needed; and $\{Q\}$) at the end of the step and for each member of the structure.

This system of equations implicitly defines a relation between the member displacements $\{q\}$ and internal forces $\{Q\}$ for each member of the structure (i.e. given a matrix $\{q\}$, the values of $\{Q\}$ can be computed by the numerical resolution of the system of equations). This relation is denoted, formally, as

$$\{Q\} = \{Q(q)\} \quad \text{or} \quad \{Q\}_b = \{Q(X)\}_b. \quad (42)$$

The last relation and the node equilibrium eqn (7) give:

$$\{L(X)\} = \{P\} - \sum_{b=1}^{m} \{Q(X)\}_b = 0. \quad (43)$$

Resolution of (43) is called the 'global problem'.

The global problem, which has only one unknown, the displacements matrix $\{X\}$, can be solved by the Newton method. In this case, this consists of the solution at each iteration 's' of the following linear problem:

$$\{L(X)\}_{s-1} + \left[\frac{\partial L}{\partial X}\right]_{s-1} (\{X\}_s - \{X\}_{s-1}) = 0,$$

where

$$\left[\frac{\partial L}{\partial X}\right] = \sum_{b=1}^{m} \left[\frac{\partial Q}{\partial q}\right]_b. \quad (44)$$

Therefore, for each global iteration, it is necessary to solve 'm' problems where, for a given value of $\{q\}$, the matrix $\{Q(q)\}$ and the contribution of each member to the global tangent matrix $[\partial L/\partial X]$ must be calculated. These are called 'local problems'.

The formulation presented in this section has the advantage that it allows the introduction of simplified damage models for frames in commercial finite element programs. Indeed, nonlinear finite element programs basically solve equations such as (43) by Newton's or other similar methods. The local problem corresponds to the calculation of an element's contribution to the global stiffness and forces matrices. Thus, the simplified damage model of a member can be included in the library of finite elements of standard structural analysis programs.

Simultaneous resolution of the global problem and the 'm' local problems is of course possible and perhaps more effective from the computational point of view. However, implementation into commercial software would be more difficult and access to the source files could be necessary.

5.4. *Numerical resolution of the local problem*

As indicated in the previous section, the local problem consists in the numerical calculation of the internal forces $\{Q\}$ and the consistent tangent matrix $[\partial Q/\partial q]$ as a function of the member displacements $\{q\}$. This can be done using the following algorithm:

(a) Calculation of generalized deformations as a function of the member deformations at the end of the step by the compatibility eqns (4).

(b) Calculation of generalized stress, internal variables and its conjugated forces as a function of the generalized deformations.

(c) Calculation of local consistent tangent matrix in 'local coordinates' $[\partial M/\partial \Phi]$ as a function of the variables computed in the steps 'a' and 'b'.

(d) Calculation of the local consistent tangent matrix in 'global coordinates' $[\partial Q/\partial q]$ as a function of the term computed in step 'c'.

(e) Calculation of the internal forces $\{Q\}$ as a function of the generalized stresses and member displacements by the member equilibrium eqns (6).

Steps 'a' and 'e' do not require further explanations since they are direct applications of the compatibility and equilibrium equations. Steps 'b', 'c' and 'd' are described in detail in the following sections.

5.5. *Calculation of the generalized stresses*

This is done by the numerical resolution of a nonlinear system of equations constituted by the stress-deformation relation (18), discretized internal variable evolution laws (39) and (40) with three unknowns: generalized stresses, internal variables and inelastic multipliers. Conjugated forces to internal variables can be expressed as a function of these variables by the state laws (24) and (25), therefore it is not necessary to include them in the local problem. The system of equations can be written as follows:

$$\{R(M, \Phi, A_k)\} = 0$$

$$\{A\}_k - \{A_0\}_k - \{T(\lambda, M, \Phi, A_k)\}_k = 0$$

$$k = 1, 2, 3, \ldots$$

$$\{V(\lambda, M, \Phi, A_k)\}_k = 0, \qquad (45)$$

where $\{A\}_1, \{A\}_2, \ldots$ represents the internal variables of the model, i.e. $\{\Phi^p\}, \{D\}, \ldots$ and

$$\{R(M, \Phi, A_k)\} = \{\Phi\} - \{\Phi^p\} - [F^d(M, D)]\{M\};$$

$$\{T(\lambda, M, \Phi, A_k)\}_k =$$

$$\begin{bmatrix} \Delta\lambda_i \left.\frac{\partial h_i}{\partial Y_i}\right|_{\{A\}=\{A_\theta\};\{Y\}=\{Y_\theta\}} \\ \Delta\lambda_j \left.\frac{\partial h_j}{\partial Y_j}\right|_{\{A\}=\{A_\theta\};\{Y\}=\{Y_\theta\}} \\ \Delta\lambda_i \left.\frac{\partial h_i}{\partial Y_n}\right|_{\{A\}=\{A_\theta\};\{Y\}=\{Y_\theta\}} + \Delta\lambda_j \left.\frac{\partial h_j}{\partial Y_n}\right|_{\{A\}=\{A_\theta\};\{Y\}=\{Y_\theta\}} \end{bmatrix}_k$$

$$\{V(\lambda, M, \Phi, A_k)\}_k = \begin{bmatrix} V_i \\ V_j \end{bmatrix}_k,$$

where

$$V_i = \begin{cases} h_i(M, \Phi, A_k) & \text{if multiplier } \lambda_i^k \text{ is active} \\ \Delta\lambda_i & \text{otherwise} \end{cases}.$$

This problem can be solved by the Newton method, however we do not know which internal variables are active and thus which expression for $\{V\}_k$ should be used. This additional difficulty arises too in plastic or viscoplastic multicriteria models of solids. The algorithms developed in these cases (see, for instance, [14]) are also applicable in the present context. We briefly describe the scheme used in the examples presented in Section 6. The algorithm can be divided into three substeps:

(a) 'Elastic predictor'. This consists of the resolution of the following subproblem:
find $\{M_e\}$ such that:

$$\{R(M_e, \Phi, A_{0k})\} = 0. \qquad (46)$$

Resolution of (46) corresponds to the computation of the generalized stresses at the end of step, assuming that there is no increment of the internal variables.

A first estimation of the set of active inelastic multipliers can now be made:
Multipliers λ_i^k is assumed active if

$$h_i(M_e, \Phi, A_{0k}) > 0. \qquad (47)$$

(b) 'Inelastic corrector'. This consists of the resolution of (45) with assumptions (47) by, for instance, the Newton method.

(c) 'Verificator-projector'. In this substep, we verify that:

(i) Each internal variable whose inelastic multiplicator is assumed active matches inequality (41) after inelastic correction. If one of them does not, then the inelastic multiplier is changed to 'passive' and a new inelastic correction is necessary.

(ii) Every yield function associated with inelastic multipliers assumed passive is negative. If one of them is not, then the inelastic multiplier is changed to 'active' and a new inelastic correction is necessary.

If no correction is needed, generalized stresses and internal variables computation is finished. These 'verification-projections' can be done at the end of the 'inelastic correction' or after each iteration during the inelastic correction [14].

5.6. *Calculation of the consistent tangent matrix in local coordinates*

Taking derivatives of eqns (45) with respect generalized deformations $\{\Phi\}$, we obtain:

$$\left[\frac{\partial R}{\partial M}\right]\left[\frac{\partial M}{\partial \Phi}\right]+\left[\frac{\partial R}{\partial A_k}\right]\left[\frac{\partial A_k}{\partial \Phi}\right]=-\left[\frac{\partial R}{\partial \Phi}\right]$$

$$\left[\frac{\partial A_k}{\partial \Phi}\right]-\left[\frac{\partial T}{\partial M}\right]\left[\frac{\partial M}{\partial \Phi}\right]-\left[\frac{\partial T}{\partial A_k}\right]\left[\frac{\partial A_k}{\partial \Phi}\right]-\left[\frac{\partial T}{\partial \lambda}\right]\left[\frac{\partial \lambda}{\partial \Phi}\right]=\left[\frac{\partial T}{\partial \Phi}\right]$$

$$\left[\frac{\partial V}{\partial M}\right]\left[\frac{\partial M}{\partial \Phi}\right]+\left[\frac{\partial V}{\partial A_k}\right]\left[\frac{\partial A_k}{\partial \Phi}\right]+\left[\frac{\partial V}{\partial \lambda}\right]\left[\frac{\partial \lambda}{\partial \Phi}\right]=-\left[\frac{\partial V}{\partial \Phi}\right]. \tag{48}$$

In this linear system of matrix equations, derivatives of generalized stresses, internal variables and inelastic multiplicators with respect to generalized deformations are the only unknowns of the problem. Resolution of (48) allows the computation of the local consistent tangent matrix in local coordinates.

5.7. *Calculation of the consistent tangent matrix in global coordinates*

Derivatives of the internal forces $\{Q\}$ with respect to member displacement $\{q\}$ can be written, taking into account eqns (6) and (3), as

$$\left[\frac{\partial Q}{\partial q}\right]=\left[\frac{\partial B^{\prime}}{\partial q}M\right]+\{B\}^{\prime}\left[\frac{\partial M}{\partial \Phi}\right][B]. \tag{49}$$

In the particular case of small displacements the first term of the consistent tangent matrix is equal to zero, since the displacement transformation matrix is constant, otherwise it can be reduced to the expression given in Appendix D.

6. NUMERICAL EXAMPLES

A program with the damage model described in Section 4 was developed using the algorithms described in Section 5 (see [8] for further details). An interface to connect this program with the finite element program ABAQUS [15] was written. Two examples processed with this program are shown in Sections 6.1 and 62.

6.1. *Collapse of a two member frame: test and numerical simulation*

The specimen represented in Fig. 10 (l = 0.455 m, area = 15 × 15 cm^2, Reinforcement 4 ϕ 9.525 mm (3/8"), $f_c' \cong 25$ N/mm^2, $f_y \cong 420$ N/mm^2) was subjected in the laboratory to the loading indicated in the same figure. Results of the test are indicated in Fig. 11. This test was modeled as a two-member structure and a numerical simulation with the program was performed. The parameters of the model were taken from the experimental results ($4EI/L$ = 17,733 kN-m, $M_u = 31.33$ kN-m, $M_p = 27.17$ kN-m, $M_{cr} = 8.49$, $\Phi_{pu} = 21.03 \times 10^{-3}$). Numerical simulation of the test is also shown in Fig. 11. Loading is represented as a concentrated force on the upper node of the frame. Collapse of the structure is reached at the same experimental value (which is not surprising since the parameters of the model were taken from the experimental results) and appeared in the calculation as the last point were a solution was founded (there is no analytical solution for force controlled simulations and arc-length algorithms have not yet been implemented in the element). Displacement controlled simulations gave the same results up to the peak of the force–displacement curve. After the peak there

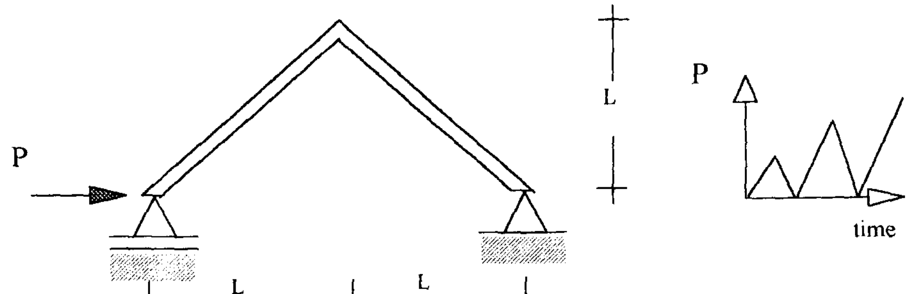

Fig. 10. Test on a two member structure: specimen and loading.

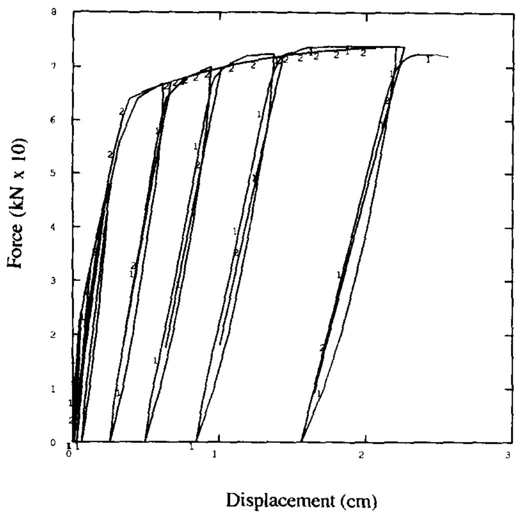

Fig. 11. Comparison between test and numerical simulation in a two member structure.

are three theoretical solutions for the first rate problem. They are not shown in the figure and uniqueness and stability analysis of the problem is not considered in this paper.

6.2. *Numerical simulation of a two storey frame's behavior*

The results of a test performed on the RC frame shown in Fig. 12 were reported in [16]. The testing first involved applying a total axial load of 700 kN to each column and maintaining this load in a force-controlled mode throughout the test. Lateral load was then applied, in a stroke-controlled mode, until the ultimate capacity of the frame was achieved. The test history in terms of applied lateral load vs deflection of the top-storey is shown in Fig. 13. In the same paper the authors reported a numerical simulation of the test (without unloading) using a multi-layer model. Forty member segments were used in the discretization and very accurate results were obtained (see [16] for details of the model and the test).

In this section we present the results of another simulation of the same test performed with the simplified damage model proposed in this paper. The structure was discretized in six members. No geometric nonlinearity was considered. The properties of the members were obtained by standard theory of reinforced concrete. Inertia and area of the cross-section were obtained by transformation of the steel area in an equivalent section of concrete. Axial loads on the columns were taken into account in the calculation of the cracking, plastic and ultimate moment of the cross-section by standard methods. Ultimate plastic rotation was calculated using the empirical expression proposed by Baker, as reported in [11]. The parameters obtained are:

Beams: $E = 26.33$ kN/mm: $I = 1.63 \times 10^9$ mm^4,

$A = 1.38 \times 10^5$ mm^2,

$M_{cr} = 0.28 \times 10^5$ kN-mm,

$M_p = 1.61 \times 10^5$ kN-mm,

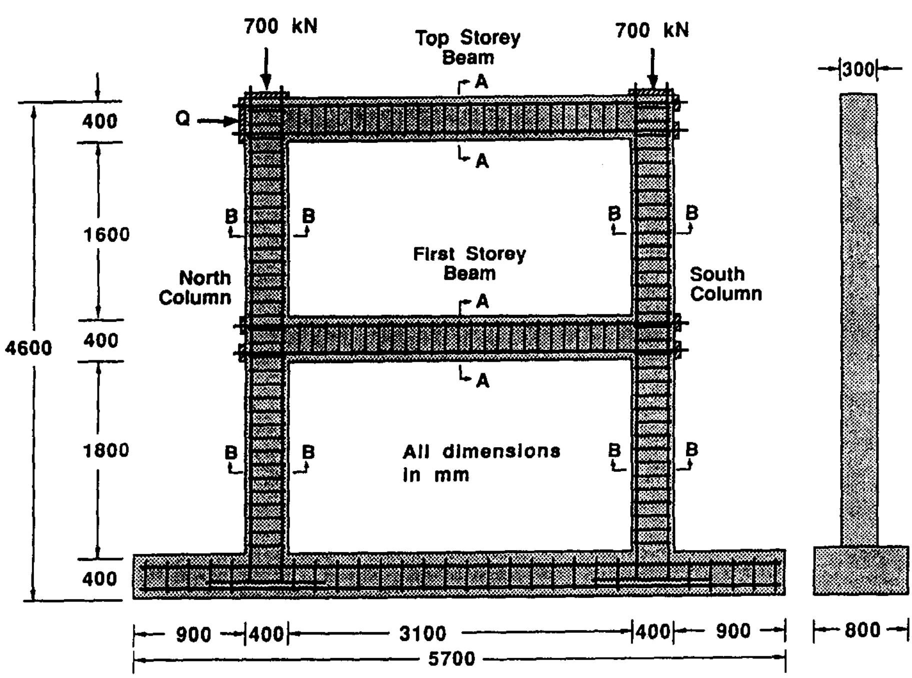

Fig. 12. Details of a test frame after [16].

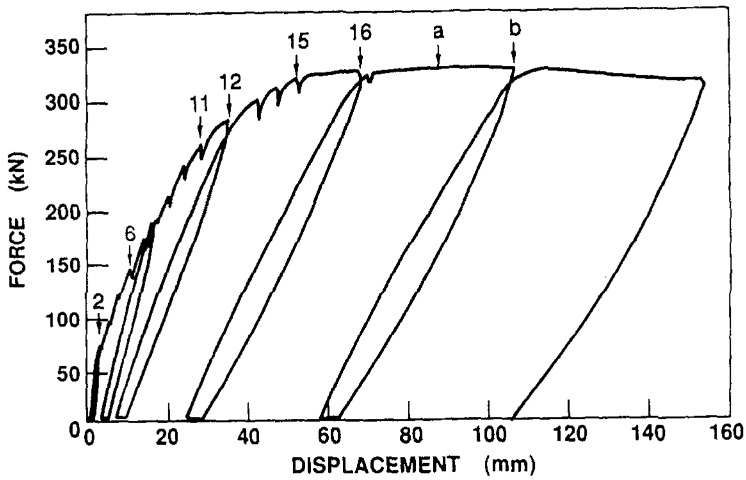

Fig. 13. Test history in terms of applied lateral load vs deflection at top-storey after [16].

$M_u = 1.89 \times 10^5$ kN-mm,

$\Phi_{pu} = 1.67 \times 10^{-2}$.

Columns: $E = 26.33$ kN-mm, $I = 1.63 \times 10^9$ mm^4,

$A = 1.38 \times 10^5$ mm^2,

$M_{cr} = 0.69 \times 10^5$ kN-mm,

$M_p = 2.53 \times 10^5$ kN-mm,

$M_u = 2.73 \times 10^5$ kN-mm,

$\Phi_{pu} = 0.6 \times 10^{-2}$.

The results of the numerical simulation are presented in Figs 14 and 15. Figure 14 indicates the force as a function of the two-storey displacement. Moment distribution at ultimate load is indicated in Fig. 15(b). The values of the damage parameters and inelastic hinges with plastic rotations at the same load are shown in Fig. 15(a).

The results are reasonably accurate, taking into account the little effort made in the calculation of the model parameters. In [16] it is reported that the frame first experienced cracking at a load of 52.5 kN and that this happened in the first storey beam at north bottom face and the south top face. In the numerical simulation, the damage variables of the first-storey beam reached positive values for the first time at a load of 51.06 kN. The values of the damage in the other members of the frame were zero at the same time. In the test, flexural cracking at the base of the columns occurred at a load of 145 kN. In the simulation, damage threshold was reached at the bottom of the columns at a load of 100 kN. The first yielding in the test is reported to occur at a load of 264 kN in the first-storey beam. Plastic deformations appeared in the simulation for the first time in the same element at load of 253 kN. Yielding at the base of columns occurred as the load approached 323 kN

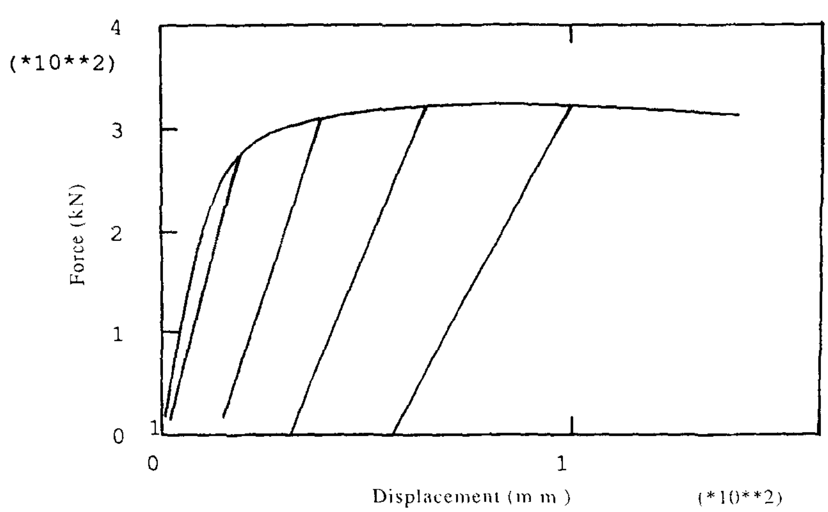

Fig. 14. Numerical simulation of the test. Lateral load vs deflection at top-storey.

(a)

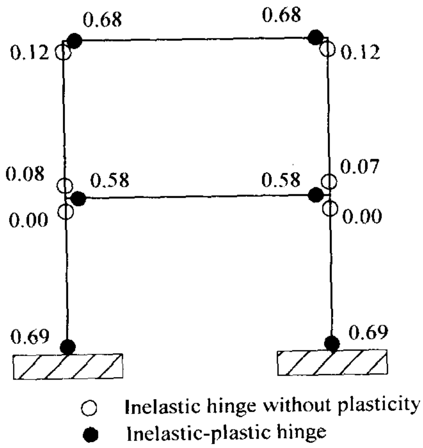

(b)

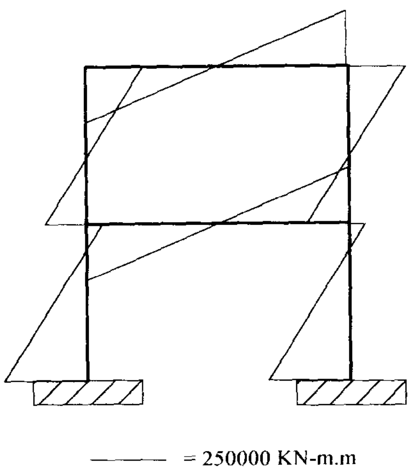

Fig. 15. State of the frame at the ultimate load. (a) Damage and plastic hinges. (b) Moment distribution.

in the test. In the simulation this happened at 296 kN. The ultimate load observed during the test was 332 kN, whereas in the simulation the ultimate load was 323 kN. The failure mechanism reported in [16] is the same as that obtained in the simulation and is indicated in Fig. 15(a).

It can be noticed that the theory of reinforced concrete gives conservative values of the parameters, therefore the model is in this case conservative. In the model, plastic deformations are assumed to occur only after the yielding of the reinforcement (since M_p was calculated in this way). In the test, non-negligible permanent deformations occurred before this, probably because of inelastic strains in the concrete and cracking. The results of the numerical simuation can be improved by taking into account this and other effects (as confinement of the concrete, dead loads and so on) in the calculation of the parameters.

These example gives an estimate of the results that an engineer could obtain by analyzing a large structure at a very low cost.

7. SUMMARY AND CONCLUSIONS

A general framework for the nonlinear analysis of frames based on the continuum damage mechanics theory and lumped dissipation models has been developed. Within this framework, many kinds of materials and loading can be taken into account. As an example, a particular model for RC frames under reversible loading was proposed and implemented into a commercial finite element program.

This simplified models seems to be an effective tool for the numerical simulation of the collapse of frames. They could be a valuable alternative when other types of analysis, such as those based on multi-layer models, appear to be too expensive or impractical due to the size and complexity of the structure.

The particular model for RC frames proposed in Section 4.6 exhibited a very high quality/price relation in the examples shown in Sections 4 and 6. The model seems very accurate if properties of the cross-section, such as inertia, plastic moment, ultimate moment and so on, can be calculated with good precision.

Simplified damage models can be implemented in commercial finite element programs with little effort. The numerical instabilities due to localization, that are typical of the strain- and damage-softening models in continuum mechanics, have not appeared in the examples treated so far.

REFERENCES

1. L. M. Kachanov, On creep rupture time. *Izv. Akad. Nauk. SSSR* **8**, 26–31 (1958).
2. J. Lemaitre and J.-L. Chaboche, *Mechanics of Solid Materials*. Dunod, Paris (1988).
3. G. Maier, L. De Donato and L. Corradi, Inelastic analysis of reinforced concrete frames by quadratic programming. *Symp. Inelasticity and Nonlinearities in Struc. Concr.*, University of Waterloo, Canada (1973).
4. Z. M. Cohn and A. Franchi, STRUPL: a computer system for structural plasticity. *J. Struc. Div. ASCE* **105**(4), 789–804 (1979).
5. P. Riva, M. Z. Cohn, Engineering approach to nonlinear analysis of concrete structures. *J. Struc. Div. ASCE* **116**(8), 2162–2185 (1989).
6. J. Flórez López, Análisis de estructuras aporticadas mediante la mecánica de la degradación (in Spanish). *Revista Internacional de Métodos Numéricos para Cálculo y Diseño en Ingeniería* **9**(2), 123–139 (1993).
7. A. Cipollina, Análisis de elementos estructurales de concreto armado mediante la mecánica de la degradación, Thesis for partial fulfillment of the requirements for the degree of Magister Scientie in Structural Engineering. University of the Andes, Mérida, Venezuela (1992) (in Spanish).
8. A. López Inojosa, Grandes desplazamientos y deformaciones en modelos simplificados de daño (in Spanish), Thesis for partial fulfillment of the requirements for the degree of Magister Scientie in Structural Engineering. University of the Andes, Mérida, Venezuela (in preparation).
9. A. Cipollina, R. Febres Cedillo and J. Flórez López, A model of plasticity coupled to damage for RC frames. *Proc. X World Conf. Earthquake Engineering*, Madrid, Spain (1992).

10. J. Flórez López, Calcul simplifié de portiques endommageables (in French). *Revue européenne des éléments finis/European Journal of Finite Elements* **2**(1), 47–74 (1993).
11. R. Park and T. Paulay, *Reinforced Concrete Structures*. John Wiley, New York. (1975) (in French).
12. M. Puglisi, Un modelo de daño por fatiga en miembros de concreto armado, Thesis for partial fulfillment of the requirements for the degree of Magister Scientie in structural engineering, University of the Andes, Mérida, Venezuela (in preparation) (in Spanish).
13. A. Benallal, Thermoviscoplasticité et endommagement des structures, Thèse de doctorat ètat. University Pierre et Marie Curie, Paris (1989) (in French).
14. J.-C. Simo, A. Kennedy and S. Govindjee, Non-smooth multisurface plasticity and viscoelasticity. Loading/unloading conditions and numerical algorithms. *Int. J. Numer. Meth. Engng* **26,** 2161–2185 (1988).
15. ABAQUS, User's manual, Hibbitt, Karlsson & Sorensen, Inc. (1988).
16. F. J. Vecchio and M. B. Emara, Shear deformations in reinforced concrete frames. *ACI Struc. J.* **89**(1) (1992).
17. H. G. Powell, Theory for nonlinear elastic structures. *J. Struc. Div. ASCE* **95** (ST12), 2687–2701 (1969).
18. Z. P. Bazant and L. Cedolin, *Stability of Structures*. Oxford University Press, New York (1991).

APPENDIX A

Displacement matrix transformation after [17]:

$$[B]=\begin{bmatrix} \frac{s}{L} & -\frac{c}{L} & 1 & -\frac{s}{L} & \frac{c}{L} & 0 \\ \frac{s}{L} & -\frac{c}{L} & 0 & -\frac{s}{L} & \frac{c}{L} & 1 \\ -c & -s & 0 & c & s & 0 \end{bmatrix},$$

where $s=\sin(\alpha)$, $c=\cos(\alpha)$, $\alpha=\alpha(t)$ is the angle between the cord of the member and the axe X and $L=L(t)$ is the length of the cord.

APPENDIX B

Relation between generalized displacements and deformations after [17]:

$$\Phi_i=q_3-(\alpha_0-\alpha(t));\quad \Phi_j=q_6-(\alpha_0-\alpha(t));$$
$$\delta=L(t)-L_0,$$

where α_0 and L_0 are the angle and length of the cord in the deformed configuration.

APPENDIX C

Flexibility matrix of a member of length L, area A and inertia I after [18]

$$[F(M)]=\frac{L}{EI}\begin{bmatrix} \Psi & \varphi & 0 \\ \varphi & \Psi & 0 \\ 0 & 0 & I/A \end{bmatrix},$$

where

$$\Psi=\begin{cases} \dfrac{1}{\tau}\left(\dfrac{1}{\tau}-\cot\tau\right) & \text{if } N\leqslant 0 \\ \dfrac{1}{\tau}\left(\dfrac{1}{\tanh\tau}-\dfrac{1}{\tau}\right) & \text{otherwise} \end{cases}$$

$$\varphi=\begin{cases} \dfrac{1}{\tau}\left(\dfrac{1}{\sin\tau}-\dfrac{1}{\tau}\right) & \text{if } N\leqslant 0 \\ \dfrac{1}{\tau}\left(\dfrac{1}{\tau}-\dfrac{1}{\sinh\tau}\right) & \text{otherwise.} \end{cases}\qquad \tau=L\sqrt{\frac{N}{EI}}$$

APPENDIX D

Term of the local consistent tangent matrix due to large displacements after [17]:

$$\left[\frac{\partial B^t}{\partial q}M\right]=\frac{N}{2}\begin{bmatrix} s^2 & -sc & 0 & -s^2 & sc & 0 \\ -sc & c^2 & 0 & sc & -c^2 & 0 \\ 0 & 0 & 0 & 0 & 0 & 0 \\ -s^2 & sc & 0 & s^2 & -sc & 0 \\ sc & -c^2 & 0 & -sc & c^2 & 0 \\ 0 & 0 & 0 & 0 & 0 & 0 \end{bmatrix}.$$